Analytical CPG model driven by single-limb velocity input generates accurate temporal locomotor dynamics

Sergiy Yakovenko Corresp., [1, 2, 3] , **Anton Sobinov** [4] , **Valeriya Gritsenko** [1, 2, 4]

[1] Department of Human Performance, School of Medicine, West Virginia University, Morgantown, WV, United States
[2] Department of Biomedical Engineering, Benjamin M. Statler College of Engineering and Mineral Resources, West Virginia University, Morgantown, WV, United States
[3] Rockefeller Neuroscience Institute, School of Medicine, WVU, West Virginia University, Morgantown, WV, United States
[4] Rockefeller Neuroscience Institute, School of Medicine, West Virginia University, Morgantown, WV, United States

Corresponding Author: Sergiy Yakovenko
Email address: seyakovenko@hsc.wvu.edu

The ability of vertebrates to generate rhythm within their spinal neural networks is essential for walking, running, and other rhythmic behaviors. The central pattern generator (CPG) network responsible for these behaviors is well-characterized with experimental and theoretical studies, and it can be formulated as a nonlinear dynamical system. The underlying mechanism responsible for locomotor behavior can be expressed as the process of leaky integration with resetting states generating appropriate phases for changing body velocity. The low-dimensional input to the CPG model generates the bilateral pattern of swing and stance modulation for each limb and is consistent with the desired limb speed as the input command. To test the minimal configuration of required parameters for this model, we reduced the system of equations representing CPG for a single limb and provided the analytical solution with two complementary methods. The analytical and empirical cycle durations were similar (R^2=0.99) for the full range of walking speeds. The structure of solution is consistent with the use of limb speed as the input domain for the CPG network. Moreover, the reciprocal interaction between two leaky integration processes was sufficient to capture fundamental experimental dynamics. This analysis provides further support for the embedded velocity or limb speed representation within spinal neural pathways involved in rhythm generation.

Analytical CPG model driven by single-limb velocity input generates accurate temporal locomotor dynamics

Sergiy Yakovenko[1,2,3*], Anton Sobinov[1], Valeriya Gritsenko[1,2,3]

[1] Rockefeller Neuroscience Institute, School of Medicine, West Virginia University, Morgantown, WV, USA

[2] Department of Human Performance, School of Medicine, West Virginia University, Morgantown, WV, USA

[3] Department of Biomedical Engineering, Benjamin M. Statler College of Engineering and Mineral Resources, West Virginia University, Morgantown, WV, USA

** Corresponding author*
E-mail: seyakovenko@hsc.wvu.edu (SY)

preprint bioRxiv doi:

Abstract

The ability of vertebrates to generate rhythm within their spinal neural networks is essential for walking, running, and other rhythmic behaviors. The central pattern generator (CPG) network responsible for these behaviors is well-characterized with experimental and theoretical studies, and it can be formulated as a nonlinear dynamical system. The underlying mechanism responsible for locomotor behavior can be expressed as the process of leaky integration with resetting states generating appropriate phases for changing body velocity. The low-dimensional input to the CPG model generates the bilateral pattern of swing and stance modulation for each limb and is consistent with the desired limb speed as the input command. To test the minimal configuration of required parameters for this model, we reduced the system of equations representing CPG for a single limb and provided the analytical solution with two complementary methods. The analytical and empirical cycle durations were similar (R^2=0.99) for the full range of walking speeds. The structure of solution is consistent with the use of limb speed as the input domain for the CPG network. Moreover, the reciprocal interaction between two leaky integration processes was sufficient to capture fundamental experimental dynamics. This analysis provides further support for the embedded velocity or limb speed representation within spinal neural pathways involved in rhythm generation.

Introduction

The mechanism of spinal rhythmogenesis is an integral part of the mammalian locomotor system that fuses descending and sensory feedback signals with body's dynamics (Dickinson et al., 2000). The theoretical description of this element, termed the central pattern generator (CPG), has been the focus of research with diverse aims. Previous computational studies introduced a variety of models to describe inter- and intra-limb coordination (Yakovenko et al., 2005; Schöner et al., 1990) and the rhythm generating network dynamics (Daun et al., 2009; Barnett and Cymbalyuk, 2014). Other models tested the organization of spinal interneuronal circuitry (Bashor, 1998; Rybak et al., 2006) and the dynamic interactions between the mechanical system and the CPG (Taga et al., 1991). The elusive mechanism of locomotor pattern generation remains to be poorly understood in the context of its regulation and integration within descending feedforward and sensory feedback pathways. One of the main obstacles is the definition of CPG's essential function. This neural element computes control commands for the redundant musculoskeletal system (Gritsenko et al., 2016) that, in turn, shapes the activity of hierarchal neural mechanisms (Lillicrap and Scott, 2013) distributed along the neuraxis (Grillner, 1985). Moreover, the spinal motor circuits are known to accommodate rewiring in healthy operation (Vahdat et al., 2015) and injured states (Stevenson et al., 2015; Liu et al., 2017).

The computational models of CPG may help to define the role of this element within the sensorimotor hierarchy. What would be the pertinent CPG model for this task? There are multiple models, and their implementation varies in complexity mostly due to the nature of addressed problems. One of the main challenges in computational neuroscience is the choice of appropriate methods and the level of abstraction for the theoretical description of complex neural mechanisms. The rule of thumb for an appropriate choice of mathematical model is to match the dexterity of experimental and theoretical descriptions. For example, the experimental data representing cellular mechanisms are captured with Hodgkin-Huxley (H-H) equations that detail the observed changes in membrane properties with the nonlinear dynamics of ion channel conductances. In contrast, the network behavior is assessed most optimally with the relatively simple phenomenological rate models that approximate the details of neural spiking by their discharge rate (Sterratt et al., 2011). Recently, the CPG models with H-H formulations were applied to cross the multiscale and multilevel divide between cellular and network levels at the cost of high parametric dimensionality but describing the underlying mechanisms responsible for neural discharge activity.

We have recently demonstrated that a bilateral CPG can represent the transformation from the desired velocity command signals to the appropriate mediation of locomotor phases in each limb (Sobinov and Yakovenko, 2017). Moreover, we have demonstrated how the asymmetric gait could be represented within the configuration of essential elements of a bilateral CPG. In contrast, our focus in this study was to test the prediction that the basic agonist-antagonist dynamical property of two coupled integrators is sufficient for the implementation of the relationship between speed and step cycle duration. For this purpose, we derived and analyzed the analytical solution of reduced single limb CPG rate model. Moreover, the general form of solution was hypothesized to be consistent with the velocity command input.

Methods

A. CPG structure and function

The observations of neural activity in the absence of descending signals or sensory feedback led T.G. Brown to formulate the principle of intrinsic rhythmogenesis of spinal networks, the half-center oscillator hypothesis (Brown, 1911). Brown posited that "… *the centres are paired, and that each pair consists of antagonistic opposites*." The intrinsic rhythmogenesis opposed the established view that the locomotor pattern is generated and shaped only by supraspinal and sensory feedback pathways. The bilateral CPG model in Fig.1 was developed from a single oscillator model to describe phase dominance in fictive cat locomotion, which is a type of experimental behavior with diminished sensory contribution (Yakovenko et al., 2005). This model controlling two limbs consisted of two dedicated oscillators made of two reciprocally coupled half-center elements (gray area in Fig.1). It can generate bilateral rhythm using the interactions within and between the half-center elements. Only the rhythm generating mechanism is captured by this feedforward rate model with time-varying inputs. The pattern formation mechanism responsible for the generation of motoneuronal input signals can be computationally decoupled from the temporal dynamics (McCrea and Rybak, 2008).

Figure 1. **The schematic of bilateral CPG.** Each locomotor phase ($T_{1\text{-}4}$) is generated by the transformation of low-feature inputs (desired velocity) with the intrinsic interactions between the half-centers (weights r_{ij}, see Eq.2). The outputs in the form of phase durations define the pattern of flexor and extensor motoneurons responsible for the activity of muscles during swing and stance for each limb.

The process of controlling phase durations is based on the ability of the network to integrate inputs until reaching a critical threshold causing a phase resetting, Fig. 2. We have previously developed the bilateral model (Yakovenko, 2011; Sobinov and Yakovenko, 2017) and describe it in brief here. The model was expressed as the system of differential equations consisting of two parts in Eq.1: *i*) the largely extrinsic signals (right side) and *ii*) the intrinsic interactions (left side). The offset term (x_0) could combine both intrinsic and extrinsic influences on the background excitability of spinal cord. The bilateral CPG model consists of a system of differential equations for four intrinsic states (x) that represent locomotor phases:

$$\dot{x} - G_x^{UL}x - G_x^{BL}(1-x)_{x>0} = x_0 + G_u u \tag{1}$$

where Gu matrix represents gains of input signals u, x_0 are constant offset values, Gx matrices represent the strength of unilateral and bilateral connections between the CPG half-centers (shown as arrows with weights r_{ij} in Fig.1). The internal states are limited to positive values with the switching threshold set to 1. Only one state from a pair, 1-2 (Fig.2) and 3-4, is set to be active $x \in (01]$ to impose the reciprocal relationship between half-centers. The unilateral (UL) and bilateral (BL) Gx matrices have the following form $G_x^{UL} = I * r_{leak}$ and

$$G_x^{BL} = \begin{bmatrix} 0 & 0 & r_{13} & r_{14} \\ 0 & 0 & r_{23} & r_{24} \\ r_{13} & r_{14} & 0 & 0 \\ r_{23} & r_{24} & 0 & 0 \end{bmatrix} \tag{2}$$

where I is the identity matrix, r_{leak} is the constant that determines intrinsic state-dependent feedback, r_{ij} are coupling terms that represent the effect between i and j elements in the model. The ascending and descending propriospinal connections crossing the midline were uncoupled in this model (r_{14}, r_{24}, r_{23}, r_{32} in Fig.1).

Even this simple model had many parameters that were largely undefined. Using an error-driven search algorithm in our previous study we found a set of optimal parameters (Table 1 in Appendix). These parameters were resolved by the minimization of the objective function with terms related to the errors in simulating swing and stance phases and the rate of their modulation for different overground speeds (Goslow et al., 1973; Halbertsma, 1983).

Results

The relationship between cycle duration and the input "drive" to the model was investigated in two complimentary solutions: *i*) the assumption of constant integration rate in a single limb model of CPG, and *ii*) the expansion of function with a Taylor series method.

Figure 2. **The temporal schematic of two reciprocal states with integration and resetting.** The integration process in flexor half-center (blue) described by Eq.3 and 7 is reset to 0 (minimal value) after reaching 1 (maximal value) and the reciprocal extensor state (red) is initiated with the same state-switching constraints.

A. Solution using constant rate assumption

First, let us simplify the equations by reducing the description only to two states controlling a single limb. Here, x_1 and x_2 are the reciprocal state variables as shown in Fig. 1. The system of equations can then be stated as:

$$\begin{cases} \dot{x}_1 = x_{01} + g_{u1}u + r_{leak}x_1 \\ \dot{x}_2 = x_{02} + g_{u2}u + r_{leak}x_2 \end{cases} \tag{3}$$

Since r_{leak} is a small negative number (Table 1) the rate of state ($\dot{x}$) can be further approximated using phase duration quantities as the difference of states for a given phase duration, i.e., the inverse of phase duration. Even for the time-variable input (u), the rate of state for a full phase duration can be simplified as:

$$\dot{x} = \frac{max - min}{\tau} = \frac{1}{\tau} \tag{4}$$

Then the expression for cycle durations can be described as a sum of the antagonistic phases in the simplified system, eq.5:

$$T_c = \tau_1 + \tau_2 = \frac{1}{\dot{x}_1} + \frac{1}{\dot{x}_2} = \frac{\dot{x}_1 + \dot{x}_2}{\dot{x}_1\dot{x}_2} \tag{5}$$

Since the cycle duration, Tc, is a constant for a given constant input (u), the only time-varying variables are the states of the system, x_1 and x_2. In phase transition points, at $t = \tau_1$ or $t = \tau_1 + \tau_2$, x_1 and x_2 are zero or a small value close to zero. We can further expand this equation with eq.3 and simplify it to all the known terms:

$$T_c = \frac{x_{01} + x_{02} + (g_{u1} + g_{u2})u}{(x_{01} + g_{u1}u)(x_{02} + g_{u2}u)} = \frac{a + bu}{\tilde{a} + \tilde{b}u + \tilde{c}u^2} \tag{6}$$

where the cycle period is expressed as a function of input (u) all parameters on the left of eq.6 are constants.

B. Solution using Taylor series

The same solution Eq.6 was found by integrating the differential equations (3) between 0 and t. For this, Eq.3 can be rewritten with the assumption of independent limb control:

$$\dot{x} - rx = x_0 + G_u u \tag{7}$$

where variables are as defined for Eq.1. Note that the right-hand side can be assumed to be time-independent for constant input (u) and this type of equations has a general solution of the form e^{kx}. The left side of the above equation can be expressed as

$$\left(xe^{-rt}\right)' = \dot{x}e^{-rt} - rxe^{-rt} = (\dot{x} - rx)e^{-rt} \tag{8}$$

Hence, Eq.7 can be integrated and evaluated between 0 and t using

$$\left(xe^{-rt}\right)\Big|_0^t = \int_0^t (x_0 + G_u u)e^{-rt}dt \tag{9}$$

$$x(t)e^{-rt} - 0 = \frac{x_0 + G_u u}{-r}\left(e^{-rt} - 1\right) \tag{10}$$

$$x(t) = \frac{x_0 + G_u u}{r}\left(e^{rt} - 1\right) \tag{11}$$

The exponential function can be further expanded with Taylor series and some components can be dropped since r is a number close to zero:

$$x(t) \approx \frac{x_0 + G_u u}{r}(1 + rt + \ldots - 1) \approx (x_0 + G_u u)t \tag{12}$$

Then, the full phase of each integrated state is

$$t = \frac{1}{x_0 + G_u u} \tag{13}$$

Finally, the full cycle duration consisting of two reciprocal phases has the same form as Eq.6

$$T_c = t_1 + t_2 = \frac{a + bu}{\tilde{a} + \tilde{b}u + \tilde{c}u^2} \tag{14}$$

where a, b, $\tilde{a}$, $\tilde{b}$, $\tilde{c}$ are constants.

C. Validation

Both methods converged on the same form, Eq. 6 and 14, supporting the consistency of solutions with different assumptions. The relationship between cycled duration and CPG input (*Tc* and *u*) is of the form $T_c=a*u^{-b}$. This simple analytical solution has a similar form to the phenomenological relationship between cycle duration and the velocity of overground forward progression $T_c=0.5445*V^{-0.5925}$ (Goslow et al., 1973). Figure 3 shows the comparison of solutions with our analytical and the previous phenomenological model for the step cycle duration and velocity values. The simulated T_c data values were calculated with Eq.7 using optimal parameters and u values selected with the regression equation $u=(V+0.1272)/0.2357$ (from Fig.4 in our previous work (Yakovenko, 2011)) and plotted in Fig.3C. The analytical solution (red) for leg speed was closely related to the empirical curve (*black*) calculated with the phenomenological functions that were calculated as the best-fit expressions for the experimental measurements (Goslow et al., 1973; Halbertsma, 1983) (Fig. 3A). The analytical and empirical cycle durations were highly correlated (Fig.3B) for the linear relationship between CPG inputs (u) representing scaled forward velocity values (Fig.3C).

Figure 3. **The comparison of analytical and empirical values.** A. The solution of cycle durations is shown for both the analytical (red) and empirical (black) values. B.The analytical cycle durations (*Tc*) are plotted as a function of empirical Tc (R^2=0.9946, $p<0.001$). C. The relationship between input signals and empirical forward velocity.

Discussion

Here, we have investigated the extreme example of the structural feedforward rate model with time-varying inputs to capture general CPG function. We have developed an analytical solution for a reduced CPG model to test if the basic structure of reciprocal interactions between integrating and leaky network elements can generate appropriate input-output relationship between limb speed and locomotor cycle duration. The analytical solution of the reduced CPG model recreated the empirical data very closely, despite model simplicity and assumptions in deriving the solution. This was not clear *a priori*. Multiple studies rely on H-H formalism and complex network with additional neurons and spinal segmental pathways to represent the relatively low-dimensional nonlinear output, which is responsible for the locomotor phase regulation.

The minimalistic implementation of CPG required significant assumptions about morphology and function in the model. Both, flexor and extensor half-centers were assumed to be capable of generating rhythm. The ability for rhythmogenesis of each half-center is the current consensus among multiple gropus {see review/ ref}, but it has been under some scrutiny, see discussion of "swing-phase" CPG below. In the model, the switching to the antagonistic phase is triggered by the state signal crossing the threshold (x_i=1). The process responsible for maintaining activity in one phase is similar to the dynamics arising from the slowly inactivating persistent sodium current in CPG models using H-H dynamics.

The dynamical rate models are appropriate for the description of the relationship between the desired speed and the locomotor phases (Fig.1). As further anatomical studies detailing the organization and wiring of neurons become available for mammalian CPG (Kiehn, 2016), the inclusion of these details in models is generally left to the intuition. H-H spike-generating models of CPG require multiple estimated parameter values that are often difficult to validate in numerical simulations. These models provide insight into the realistic control challenges and reveal tentative explanations of experimental discrepancies. For example, the discrepancy between the observation of both extensor and flexor phase dominance in locomotor patterns generated by adaptable flexor- and extensor- driven CPG as opposed to only the flexor-driven CPG (see review/ Duysens et al., 2013) can be reconciled with the consideration of available functionality within underlying single-cell and network dynamic elements (Ausborn et al., 2017). A subset of plausible mechanisms selected from the plethora of unexplored parametric relationships can explains multiple observed states, and other alternative mechanisms generating similar outcomes may exist within the same models.

The evidence of underfitting of experimental data by simple models should be the main motivation for the inclusion of additional terms within theoretical representations. As we have observed in a relatively complex dynamical rate model simulating asymmetric bilateral locomotion (Sobinov and Yakovenko, 2017), the same low-dimensional output can be produced by several alternative parameter configurations. What region of the parameter space, which is nine-dimensional for a bilateral rate model, is physiological remains to be established. The potential of dynamical rate models to simulate brain functions also remains an open question. Their utility was demonstrated in a series of studies of motor cortical processing spanning reaching movements and motor learning (Churchland et al., 2012; Gilja et al., 2012; Kao et al., 2015; Sussillo et al., 2015). Our finding suggests that dynamical rate models solve the problem of transforming high-level commands by capturing empirical observations of temporal phase relationships.

The presented solution is based on the analysis of a single limb controller. How does this apply to the behaviors with the interlimb contributions? In a quadruped, the CPG is a network of all four limb controllers that generate patterns with the inputs of all its elements. The analyses of locomotor patterns in split-belt locomotion, when fore- and hind- limbs or left and right limbs were decoupled and allowed to move at different speeds, support the idea that forelimb and hindlimb CPGs are similarly organized without midline asymmetries (D'Angelo et al., 2014). The upper and lower limb CPG networks have been proposed to monitor and to integrate sensory inputs with the ongoing rhythmic activity both in cats and also in humans (Duysens and Van de Crommert HW, 1998). For example, the cutaneous inputs are similarly modulated in lower limbs during locomotion and in upper limbs during rhythmic, cyclical arm tasks (Zehr and Kido, 2001). The similarity in the structure of the upper and lower limb controllers and their symmetricity across the midline corroborates the idea that the understanding of single limb CPG dynamics is central to the description of inter limb coordination and sensorimotor integration. Thus, this model may be adapted in the future studies to capture, at least partially, upper-limb dynamics in rhythmic movements.

The computational complexity of motor control can be reduced by generating commands through a selection of independent control units, *synergies*, that combine muscles to produce desired mechanical actions (Saltiel et al., 2001). This Bernsteinian problem could be solved by the basic CPG structure capturing the temporal features of bilateral muscle activity during locomotion. By definition, CPG function constitutes a locomotor synergy; yet, the current methods for studying motor synergies are generally linear statistical tools (Tresch and Jarc, 2009). The typical factorization methods, i.e., the nonnegative matrix factorization, would not identify CPG as a single synergy and, moreover, would require an additional mechanism to modulate locomotor phases with speed. The CPG model described here is a compact and robust alternative, which is supported by the recent use of dynamical systems in the description of control pathways. The dynamical systems can characterize the transformation from neural activity in the primary motor cortex to the muscle activations controlling reaching movements (Sussillo et al., 2015) or in the preparatory activity of premotor areas planning these commands (Kaufman et al., 2014).

The description of mechanisms responsible for the coordination of phasic activity during locomotion may be necessary for the development of stroke and spinal cord injury repair and rehabilitation strategies (Thompson, 2012). The basic mechanistic description of CPG is critical for the development of robotic and clinical applications that take advantage of this element, and it is essential for the functional understanding of hierarchical descending and sensory feedback pathways projecting to it. The fundamental dynamical form of CPG mechanism and its validation in locomotion with different velocities opens a robust alternative to computationally intensive models.

Conclusion

The analytical solution demonstrates that the linear relationship between forward velocity or limb speed is the essential property of reciprocal organization between two half-center oscillators in this CPG model. Moreover, there is a good correspondence between the form of analytical solution and the previous empirical description of this relationship. The existence of rhythmogenic neural networks with the reciprocal inhibition makes it possible to use gross signals, i.e. limb velocity, to specify the nonlinear regulation of locomotor phases. Further theoretical description of CPG may provide tools for intelligent prosthetics and the quantitative metrics of locomotor disabilities.

Appendix

Table 1. Optimal CPG parameters from Yakovenko (2011).

Parameter	x_{01}	x_{02}	g_1	g_2	r_{leak}	r_{13}	r_{14}	r_{23}	r_{24}
Value	-0.0007	2.4256	0.6203	0.4882	-0.0094	0.1339	-0.0485	-0.0823	0.0981

Acknowledgements

We thank Jonathan E. Rubin for the discussion of analytical models that led to the development of this paper. This work was supported by a student fellowship National Institute of Health, T32, AG052375-01A1 (AS), salary support from National Institute of Health, National Institute of General Medical Sciences, P20GM109098 (SY, VG), and administrative support U54GM104942 (SY). *The funders had no role in study design, data collection and analysis, decision to publish, or preparation of the manuscript.*

Figure Legends

Fig. 1. **The schematic of bilateral CPG.** Each locomotor phase *Ti* is generated by the transformation of low-feature inputs (desired velocity) with the intrinsic interactions between the

half-centers (weights r_{ij}, see Eq.2). The outputs in the form of phase durations define the pattern of flexor and extensor motoneurons responsible for the activity of muscles during swing and stance for each limb.

Fig. 2. **The temporal schematic of two reciprocal states with integration and resetting.** The integration process in flexor half-center (blue) described by Eq.3 and 7 is reset to 0 and the reciprocal extensor state (red) is initiated.

Fig. 3. **The comparison of analytical and empirical values.** A. The solution of cycle durations is shown for both the analytical (red) and empirical (black) values. B. The analytical cycle durations (Tc) are plotted as a function of empirical Tc (R^2=0.9946, $p<0.001$). C. The relationship between input signals and empirical forward velocity.

References

Ausborn J, **Snyder AC**, **Shevtsova NA**, **Rybak IA**, **Rubin JE**. State-Dependent Rhythmogenesis and Frequency Control in a Half-Center Locomotor CPG. *J Neurophysiol* 119: jn.00550.2017–117, 2017.

Barnett WH, **Cymbalyuk GS**. A codimension-2 bifurcation controlling endogenous bursting activity and pulse-triggered responses of a neuron model. *PLoS ONE* 9: e85451, 2014.

Bashor DP. A large-scale model of some spinal reflex circuits. *Biol Cybern* 78: 147–157, 1998.

Brown TG. The intrinsic factors in the act of progression in the mammal. *P Roy Soc B-Biol Sci* 84: 308–319, 1911.

Churchland MM, **Cunningham JP**, **Kaufman MT**, **Foster JD**, **Nuyujukian P**, **Ryu SI**, **Shenoy KV**. Neural population dynamics during reaching. *Nature* 487: 51–56, 2012.

D'Angelo G, **Thibaudier Y**, **Telonio A**, **Hurteau M-F**, **Kuczynski V**, **Dambreville C**, **Frigon A**. Modulation of phase durations, phase variations, and temporal coordination of the four limbs during quadrupedal split-belt locomotion in intact adult cats. *J Neurophysiol* 112: 1825–1837, 2014.

Daun S, **Rubin JE**, **Rybak IA**. Control of oscillation periods and phase durations in half-center central pattern generators: a comparative mechanistic analysis. *J Comput Neurosci* 27: 3–36, 2009.

Dickinson MH, **Farley CT**, **Full RJ**, **Koehl MA**, **Kram R**, **Lehman S**. How animals move: an integrative view. *Science* 288: 100–106, 2000.

Duysens J, **De Groote F**, **Jonkers I**. The flexion synergy, mother of all synergies and father of new models of gait. *Front Comput Neurosci* 7: 14, 2013.

Duysens J, **Van de Crommert HW**. Neural control of locomotion; Part 1: The central pattern generator from cats to humans. *Gait Posture* 7: 131–141, 1998.

PeerJ Preprints | https://doi.org/10.7287/peerj.preprints.26734v1 | CC BY 4.0 Open Access | rec: 19 Mar 2018, publ: 19 Mar 2018

Gilja V, **Nuyujukian P**, **Chestek CA**, **Cunningham JP**, **Yu BM**, **Fan JM**, **Churchland MM**, **Kaufman MT**, **Kao JC**, **Ryu SI**, **Shenoy KV**. A high-performance neural prosthesis enabled by control algorithm design. *Nat Neurosci* 15: 1752–1757, 2012.

Goslow GE, **Reinking RM**, **Stuart DG**. The cat step cycle: hind limb joint angles and muscle lengths during unrestrained locomotion. *J Morphol* 141: 1–41, 1973.

Grillner S. Neurobiological bases of rhythmic motor acts in vertebrates. *Science* 228: 143–149, 1985.

Gritsenko V, **Hardesty RL**, **Boots MT**, **Yakovenko S**. Biomechanical Constraints Underlying Motor Primitives Derived from the Musculoskeletal Anatomy of the Human Arm. *PLoS ONE* 11: e0164050, 2016.

Halbertsma JM. The stride cycle of the cat: the modelling of locomotion by computerized analysis of automatic recordings. *Acta Physiol Scand Suppl* 521: 1–75, 1983.

Kao JC, **Nuyujukian P**, **Ryu SI**, **Churchland MM**, **Cunningham JP**, **Shenoy KV**. Single-trial dynamics of motor cortex and their applications to brain-machine interfaces. *Nat Commun* 6: 7759, 2015.

Kaufman MT, **Churchland MM**, **Ryu SI**, **Shenoy KV**. Cortical activity in the null space: permitting preparation without movement. *Nat Neurosci* 17: 440–448, 2014.

Kiehn O. Decoding the organization of spinal circuits that control locomotion. *Nat Rev Neurosci* 17: 224–238, 2016.

Lillicrap TP, **Scott SH**. Preference distributions of primary motor cortex neurons reflect control solutions optimized for limb biomechanics. *Neuron* 77: 168–179, 2013.

Liu Y, **Wang X**, **Li W**, **Zhang Q**, **Li Y**, **Zhang Z**, **Zhu J**, **Chen B**, **Williams PR**, **Zhang Y**, **Yu B**, **Gu X**, **He Z**. A Sensitized IGF1 Treatment Restores Corticospinal Axon-Dependent Functions. *Neuron* 95: 817–833.e4, 2017.

McCrea DA, **Rybak IA**. Organization of mammalian locomotor rhythm and pattern generation. *Brain Res Rev* 57: 134–146, 2008.

Rybak IA, **Shevtsova NA**, **Lafreniere-Roula M**, **McCrea DA**. Modelling spinal circuitry involved in locomotor pattern generation: insights from deletions during fictive locomotion. *J Physiol* 577: 617–639, 2006.

Saltiel P, **Wyler-Duda K**, **d'Avella A**, **Tresch MC**, **Bizzi E**. Muscle synergies encoded within the spinal cord: evidence from focal intraspinal NMDA iontophoresis in the frog. *J Neurophysiol* 85: 605–619, 2001.

Schöner G, **Jiang WY**, **Kelso JA**. A synergetic theory of quadrupedal gaits and gait transitions. *J Theor Biol* 142: 359–391, 1990.

Sobinov A, **Yakovenko S**. Model of a bilateral Brown-type central pattern generator for symmetric and asymmetric locomotion. *J Neurophysiol* (November 29, 2017). doi: 10.1152/jn.00443.2017.

Sterratt D, **Graham B**, **Gillies A**, **Willshaw D**. *Principles of Computational Modelling in Neuroscience*. Cambridge University Press, 2011.

Stevenson AJ, **Mrachacz-Kersting N**, **van Asseldonk E**, **Turner DL**, **Spaich EG**. Spinal plasticity in robot-mediated therapy for the lower limbs. *Journal of neuroengineering and rehabilitation* 12: 81, 2015.

Sussillo D, **Churchland MM**, **Kaufman MT**, **Shenoy KV**. A neural network that finds a naturalistic solution for the production of muscle activity. *Nat Neurosci* 18: 1025–1033, 2015.

Taga G, **Yamaguchi Y**, **Shimazu H**. Self-organized control of bipedal locomotion by neural oscillators in unpredictable environment. *Biol Cybern* 65: 147–159, 1991.

Thompson AK. Interlimb coordination during locomotion: finding available neural pathways and using them for gait recovery. *Clin Neurophysiol* 123: 635–637, 2012.

Tresch MC, **Jarc A**. The case for and against muscle synergies. *Curr Opin Neurol* 19: 601–607, 2009.

Vahdat S, **Lungu O**, **Cohen-Adad J**, **Marchand-Pauvert V**, **Benali H**, **Doyon J**. Simultaneous Brain-Cervical Cord fMRI Reveals Intrinsic Spinal Cord Plasticity during Motor Sequence Learning. *PLoS Biol* 13: e1002186, 2015.

Yakovenko S, **McCrea DA**, **Stecina K**, **Prochazka A**. Control of locomotor cycle durations. *J Neurophysiol* 94: 1057–1065, 2005.

Yakovenko S. A hierarchical perspective on rhythm generation for locomotor control. *Prog Brain Res* 188: 151–166, 2011.

Zehr EP, **Kido A**. Neural control of rhythmic, cyclical human arm movement: task dependency, nerve specificity and phase modulation of cutaneous reflexes. *J Physiol* 537: 1033–1045, 2001.

Figure 1(on next page)

The schematic of bilateral CPG.

Each locomotor phase *Ti* is generated by the transformation of low-feature inputs (desired velocity) with the intrinsic interactions between the half-centers (weights r_{ij}, see Eq.2). The outputs in the form of phase durations define the pattern of flexor and extensor motoneurons responsible for the activity of muscles during swing and stance for each limb.

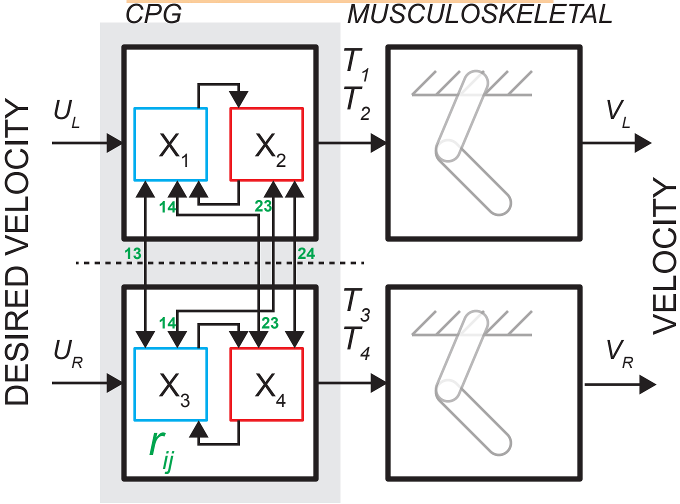
CPG
MUSCULOSKELETAL
DESIRED VELOCITY
U_L
U_R
X_1
X_2
X_3
X_4
14
23
13
24
14
23
r_{ij}
T_1
T_2
T_3
T_4
V_L
V_R
VELOCITY

Figure 2(on next page)

The temporal schematic of two reciprocal states with integration and resetting.

The integration process in flexor half-center (blue) described by Eq.3 and 7 is reset to 0 and the reciprocal extensor state (red) is initiated.

PeerJ Preprints | https://doi.org/10.7287/peerj.preprints.26734v1 | CC BY 4.0 Open Access | rec: 19 Mar 2018, publ: 19 Mar 2018

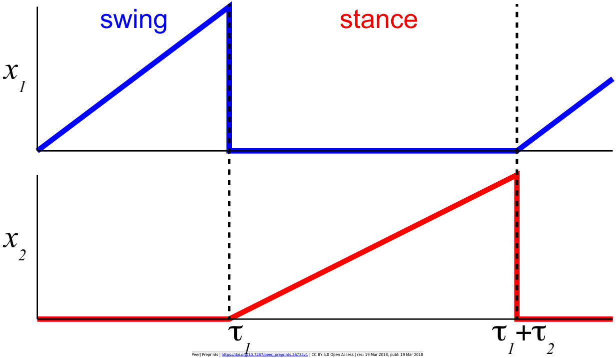
swing
stance
x_1
x_2
τ_1
$\tau_1+\tau_2$

Figure 3 (on next page)

The comparison of analytical and empirical values.

A. The solution of cycle durations is shown for both the analytical (red) and empirical (black) values. B. The analytical cycle durations (Tc) are plotted as a function of empirical Tc (R^2=0.9946, $p<0.001$). C. The relationship between input signals and empirical forward velocity.

PeerJ Preprints | https://doi.org/10.7287/peerj.preprints.26734v1 | CC BY 4.0 Open Access | rec: 19 Mar 2018, publ: 19 Mar 2018

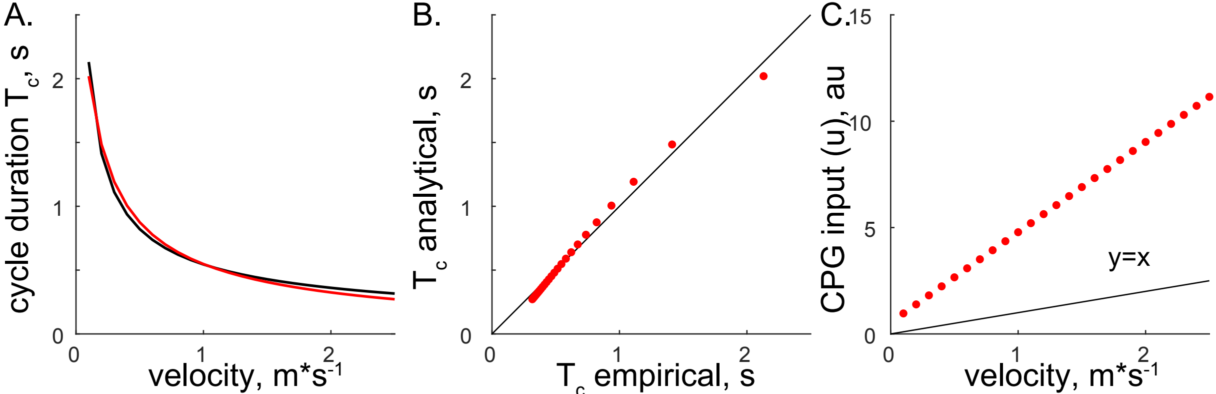
A.
cycle duration T_c, s
velocity, m*s^{-1}
B.
T_c analytical, s
T_c empirical, s
C.
CPG input (u), au
y=x
velocity, m*s^{-1}

Table 1(on next page)

Optimal CPG parameters

The parameter values were selected from Yakovenko (2011).

Table 1. Optimal CPG parameters from Yakovenko (2011).

Parameter	x_{01}	x_{02}	g_1	g_2	r_{leak}	r_{13}	r_{14}	r_{23}	r_{24}
Value	-0.0007	2.4256	0.6203	0.4882	-0.0094	0.1339	-0.0485	-0.0823	0.0981